ACS APPLIED MATERIALS & INTERFACES

Research Article

www.acsami.org

Spiropyran-Modified Gold Nanoparticles: Reversible Size Control of Aggregates by UV and Visible Light Irradiations

Yasuhiro Shiraishi,*[,†] Eri Shirakawa,[†] Kazuya Tanaka,[†] Hirokatsu Sakamoto,[†] Satoshi Ichikawa,[‡] and Takayuki Hirai[†]

[†]Research Center for Solar Energy Chemistry and Division of Chemical Engineering, Graduate School of Engineering Science, Osaka University, Toyonaka 560-8531, Japan

[‡]Institute for NanoScience Design, Osaka University, Toyonaka 560-8531, Japan

Supporting Information

ABSTRACT: UV or visible light irradiation of gold nanoparticles (AuNPs) modified with a thiol-terminated spiropyran dye promotes reversible aggregation or dispersion of AuNPs. This is facilitated by the electrostatic repulsion/attraction between the AuNPs controlled by the ring-opening/closing photoisomerization of the surface dyes. This photochemical method successfully produces aggregates of AuNPs with tunable sizes (20−340 nm) and narrow size distributions (standard deviation <34%) in a reversible manner. In addition, the formed aggregates, even when left in the dark condition, scarcely change their sizes because the stacking interaction between the ring-opened forms of surface dyes suppresses thermal reverse isomerization and maintains the attractive force between the AuNPs.

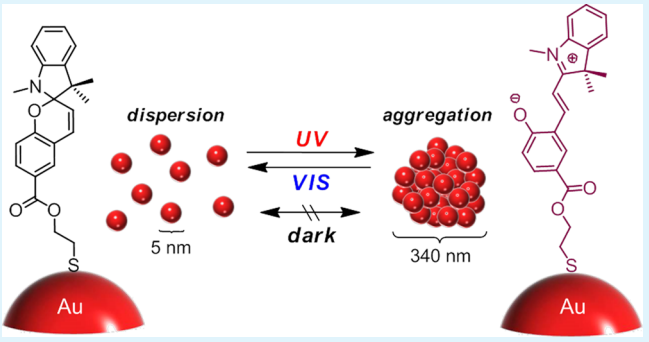

KEYWORDS: *gold nanoparticles, self-assembly, spiropyran, photoisomerization, aggregation*

1. INTRODUCTION

Gold nanoparticles (AuNPs) are unique building blocks with sophisticated optical,[1] electromagnetic,[2] and chemical[3] properties that differ dramatically from those of bulk metal. They have tremendous potentials for cancer diagnosis, therapy, and imaging because of their surface plasmon resonance (SPR) enhanced light scattering and absorption properties.[4] Due to the high surface-to-volume ratio and high surface energy, AuNPs exhibit unusual catalytic[5] and photocatalytic activities[6,7] as well as electrochemical properties.[8] These properties strongly depend on the size of AuNPs;[9] therefore, accurate size control of AuNPs is a challenge for advanced processing.

Self-assembly of AuNPs is one powerful method for size control, a simple and low-cost method to produce ensembles of AuNPs in a controllable manner.[10−12] Light-triggered methods have been studied extensively[13−27] because light is noninvasive and can be delivered instantaneously to the whole volume of sample without any transport limitations inherent to the delivery of chemicals. These methods usually employ AuNPs modified with covalently bound photoresponsive molecules. These AuNPs, when left in the dark condition, are well dispersed in solution due to the electrostatic repulsion between the AuNPs. Photoactivation of the surface molecules changes the surface electronic charge or the particle geometry, thus promoting aggregation of AuNPs. Several photoreactions have been proposed for this purpose; however, many of them are irreversible.[19−24] Creation of light-triggered method that facilitates reversible aggregation/dispersion of AuNPs is therefore the current focus of attention for size control of AuNPs.

One of the most important applications of light-triggered reversible aggregation/dispersion of AuNPs is the "on/off" switching of their catalytic activity proposed by Grzybowski's group.[28] This system uses azobenzene-modified AuNPs, which undergo reversible aggregation/dispersion by UV or visible light irradiation based on photoisomerization of the surface azobenzene dyes.[13−19] The trans form of azobenzenes possesses a small dipole moment. The AuNPs, when left in the dark condition, are well dispersed in solution due to the electrostatic repulsion between the AuNPs. The high surface area of the AuNPs therefore exhibits high catalytic activity for hydrosilylation of aldehyde. UV irradiation promotes isomerization of the azobenzene moiety to the cis form with a large dipole moment. This decreases the electrostatic repulsion between the AuNPs and promotes aggregation. The aggregated AuNPs with decreased surface area therefore switches the catalytic activity off. In contrast, visible light irradiation of the aggregates leads to cis → trans isomerization and promotes

Received: February 12, 2014
Accepted: April 18, 2014
Published: April 18, 2014

redispersion of AuNPs, thus regaining high catalytic activity. The azobenzene−AuNPs system is therefore potentially applicable for reversible on/off switching of catalytic activity by simple light stimuli without tedious heating/cooling of the solution.

Literature has described aggregation/dispersion properties of azobenzene-modified AuNPs under UV or visible light irradiation. It has been clarified that the cis → trans isomerization of the azobenzene moiety also occurs thermally even in the dark condition.[13−20] The aggregated AuNPs, when left in the dark condition, undergo spontaneous redispersion; therefore, a clear "on/off switching" of their catalytic activity cannot be attained. To the best of our knowledge, there is no report of light-triggered method that promotes reversible size control of AuNPs "just" by UV or visible light irradiation while maintaining their sizes in the dark condition.

The purpose of this work is the discovery of AuNPs, which promotes aggregation/dispersion just by photoirradiation while maintaining their sizes in the dark condition. Herein, we report that the use of a spiropyran dye is one possible way for this purpose. As shown in Scheme 1, these dyes belong to a class of

Scheme 1. Photoisomerization of Spiropyran Dyes

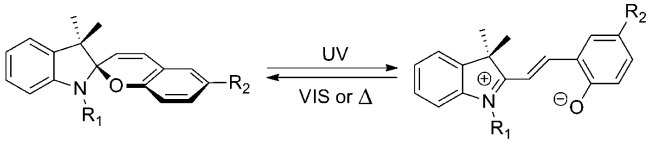

organic photochromes, which undergo ring-opening/closing isomerization between the spirocyclic (SP) form and the merocyanine (MC) form upon UV or visible light irradiation.[29−31] Several kinds of materials have been synthesized based on the photoisomerization properties.[32] The SP form has a small dipole moment, whereas the MC form has a large dipole moment due to its charge-separated state.[33] We prepared AuNPs modified with a thiol-terminated spiropyran (**1**). As shown in Scheme 2, UV irradiation of the **1**-modified AuNPs (**1**-AuNPs) promotes aggregation due to the large dipole moment of the photoformed surface MC forms. In contrast, visible light irradiation of the aggregates leads to redispersion by the MC → SP reversion. A noticeable feature of this system is that the formed aggregates maintain their sizes even when left in the dark condition. This is because, as shown in Scheme 2 (bottom), the stacking interaction between the surface MC forms suppresses thermal MC → SP reversion and maintains electrostatic attraction between the AuNPs. This simple spiropyran system successfully produces AuNPs aggregates with tunable sizes (20−340 nm) and narrow size distributions (standard deviation <34%).

2. RESULTS AND DISCUSSION

2.1. Synthesis and Properties of 1. Compound **1** was synthesized by two step reactions as shown in Scheme 3. Condensation of 1,3,3-trimethyl-2-methylideneindole (**2**)[34] and 3-formyl-4-hydroxybenzoic acid (**3**)[35] gave **4** as a red solid with 70% yield. Esterification of **4** with 2-mercaptoethanol gave **1** with 18% yield. The purity of **1** was confirmed by ^{1}H, ^{13}C NMR, and EI-MS analysis (Figures S1−S3, Supporting Information).

Scheme 2. Mechanism for Light-Triggered Reversible Aggregation/Dispersion of AuNPs Modified with a Spiropyran Dye (1)

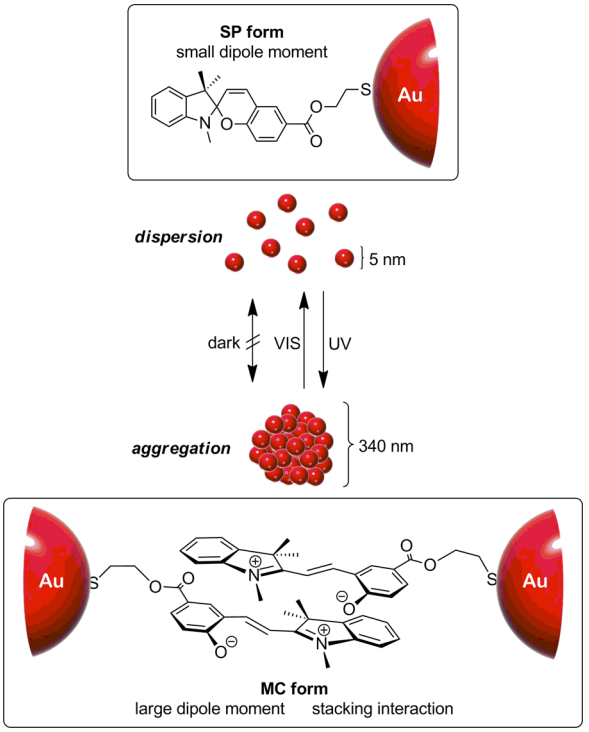

Scheme 3. Synthesis of 1[a]

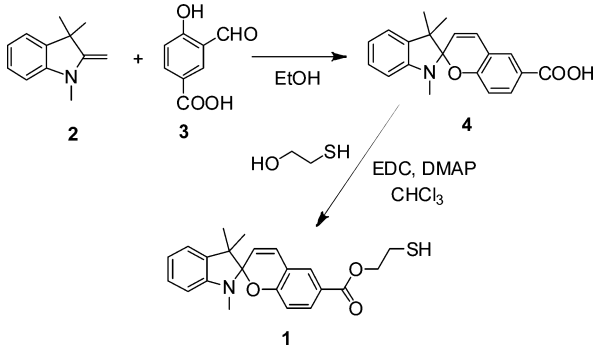

[a]EDC, 1-ethyl-3-(3-dimethylaminopropyl) carbodiimide hydrochloride; DMAP, *N*,*N*-dimethyl-4-aminopyridine.

Figure 1a shows the time-dependent change in absorption spectra of **1** (20 μM) measured in a water/MeCN mixture (1/1 v/v) at 25 °C. In the dark condition (blue line), **1** shows almost no absorption at >400 nm, indicating that **1** exists as a SP form (Scheme 1).[34] UV irradiation (300 nm) of the solution, however, creates a distinctive absorption band at 530 nm, assigned to the MC form,[36] suggesting that SP → MC isomerization indeed occurs upon UV irradiation. The isomerization yield at the photostationary state was roughly determined to be ca. 70% based on the change in absorbance at 247 nm.[37] As shown in Figure 1b, the sample containing the MC form, when left in the dark at 25 °C, shows a decrease in the MC band, along with a formation of the SP band. This indicates that, as shown in Scheme 1, the MC form of **1** is thermally reverted to the SP form, as observed for related spiropyran dyes.[38] In contrast, as shown in Figure 1c, visible light (540 nm) irradiation to the solution containing the MC

dx.doi.org/10.1021/am5009002 | ACS Appl. Mater. Interfaces 2014, 6, 7554−7562

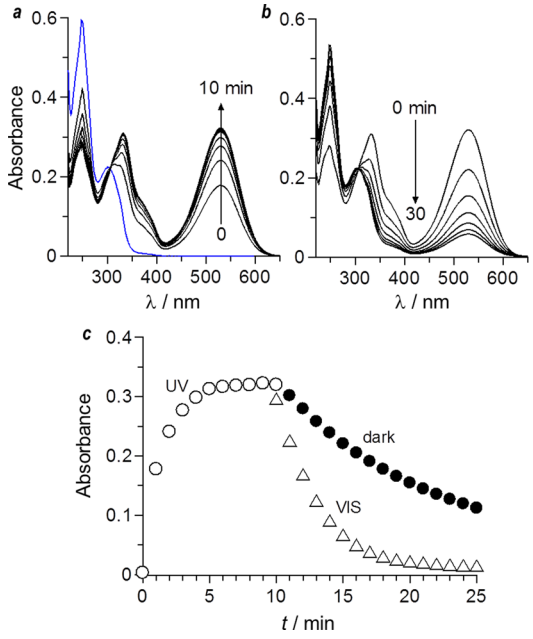

Figure 1. Absorption spectra of **1** (20 μM) in a water/MeCN mixture (1/1 v/v; HEPES 0.1 M, pH 7.0), measured at 25 °C (a) upon UV irradiation (300 nm) and (b) in the dark condition. (c) Time-dependent change in the absorbance at 530 nm during UV irradiation followed by visible light (540 nm) irradiation. The blue line in panel a is the spectrum of **1** measured in the dark.

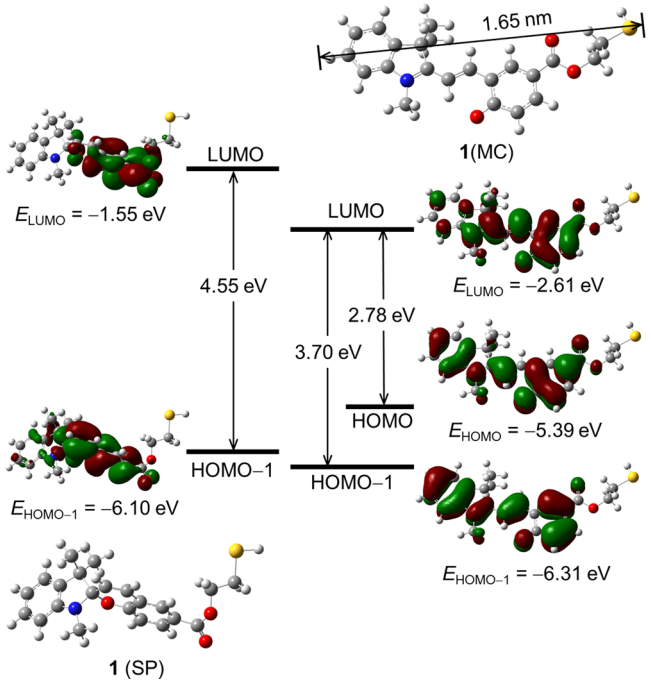

Figure 2. Energy diagrams and interfacial plots of key molecular orbitals for the SP and MC forms of **1**, calculated at the DFT level (B3LYP/6-31G).

form decreases the MC band with a rate much faster than that in the dark condition. This indicates that, as shown in Scheme 1, the MC → SP reversion is indeed promoted by visible light irradiation. In addition, as shown in Figure S4 (Supporting Information), repeated irradiation of UV and visible light successfully promotes sequential formation of the MC and SP forms. These data suggest that UV and visible light irradiations successfully promotes reversible photoisomerization of **1**.

The formation of the SP and MC forms is confirmed by ab initio calculation based on the density functional theory (DFT) within the Gaussian 03 program.[39] Table 1 summarizes the electronic transition properties of the SP and MC forms of **1**, determined by the time-dependent DFT calculation. The interfacial plots of key molecular orbitals are depicted in Figure 2. Singlet electronic excitation of the SP form of **1** is mainly contributed by HOMO−1 → LUMO ($S_0 \rightarrow S_3$) transition (302 nm), which is close to the observed absorption maximum (300 nm, Figure 1). In contrast, the excitation of the MC form of **1** is contributed by HOMO → LUMO ($S_0 \rightarrow S_1$, 488 nm) and HOMO−1 → LUMO ($S_0 \rightarrow S_3$, 374 nm) transitions, which are also close to the observed absorption maxima (529 and 333 nm, respectively). These data suggest that the calculated results precisely represent the electronic properties of the SP and MC forms. As summarized in Table 1, total dipole moment of the SP form is determined to be 5.1 D, whereas that of the MC form is 14.8 D. This suggests that the MC form indeed possesses a larger dipole moment, as observed for related spiropyran derivatives.[33]

2.2. Preparation of 1-Modified AuNPs. AuNPs were prepared by the Brust method with tetraoctylammonium bromide (TOAB) as a surface stabilizing agent.[15,26,40] An aqueous $HAuCl_4$ (0.17 mg, 12 μmol) solution (1 mL) was added to a toluene solution (2.5 mL) containing TOAB (13 mg, 24 μmol). The mixture was stirred for 10 min at 25 °C, and the colorless aqueous phase was removed. An aqueous $NaBH_4$ (2.8 mg, 74 μmol) solution (1 mL) was added slowly to the resulting toluene solution, and the mixture was stirred vigorously at 25 °C for 3 h. Water was added to the mixture, and the aqueous phase was removed, affording a dark-red toluene solution containing AuNPs stabilized with TOAB. **1** (2.3 mg, 6 μmol) was added to the obtained toluene solution and stirred vigorously at 25 °C for 3 h, giving rise to **1**-modified AuNPs (**1**-AuNPs). UV−vis analysis of the supernatant

Table 1. Calculated Dipole Moments and Electronic Excitation Properties for the SP and MC Forms of 1[a]

	μ/D							
species	μ_x	μ_y	μ_z	μ_{total}		CIC[b]	E/eV [λ/nm]	f
1(SP)	−2.97	3.65	2.01	5.12	$S_0 \rightarrow S_1$	HOMO → LUMO (0.685)	3.3736 [367.51]	0.0423
					$S_0 \rightarrow S_2$	HOMO → LUMO+1 (0.685)	3.6752 [337.35]	0.0040
					$S_0 \rightarrow S_3$	HOMO−1 → LUMO (0.617)	4.1025 [302.22]	0.1962
1(MC)	−13.96	−4.79	0.20	14.76	$S_0 \rightarrow S_1$	HOMO → LUMO (0.619)	2.5395 [488.22]	0.9036
					$S_0 \rightarrow S_2$	HOMO−2 → LUMO (0.688)	2.7329 [453.68]	0.0000
					$S_0 \rightarrow S_3$	HOMO−1 → LUMO (0.652)	3.3123 [374.32]	0.2905

[a]Calculated at the DFT level (B3LYP/6-31G). [b]CI expansion coefficients for the main orbital transitions.

obtained by centrifugation of the AuNPs solution scarcely detected the compound **1**, suggesting that all of the **1** molecules added (100 μM) are attached onto the AuNPs surface. The quantity of **1** attached onto the single spherical AuNP (49 nM) is therefore calculated to be 2.0×10^3 molecules.

The **1** molecules are covalently attached onto the Au surface through the Au−S bonding. This is confirmed by X-ray photoelectron spectroscopy (XPS). Figure 3 shows the XPS

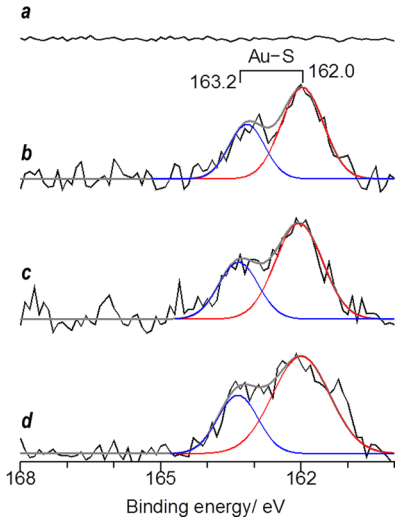

Figure 3. XPS chart (S 2p region) for (a) unmodified AuNPs and (b) **1**- AuNPs. The panel c is obtained after UV irradiation of **1**-AuNPs. The panel d is obtained after visible light irradiation of the aggregated **1**-AuNPs (sample c).

charts for S 2p signals. Unmodified AuNPs (Figure 3a) show almost no signals. In contrast, as shown in Figure 3b, **1**-AuNPs exhibit characteristic doublet at 162.0 and 163.2 eV with areas in the ratio 2:1, assigned to a thiol bound to the AuNPs surface.[41,42] This indicates that, as shown in Scheme 2, the **1** molecules are indeed bound to the Au surface through the Au−S bond formation.

2.3. Aggregation of 1-AuNPs upon UV Irradiation. Figure 4 shows the time-dependent change in the absorption spectra of the toluene solution containing **1**-AuNPs measured at 25 °C. As shown by the red line (Figure 4a), the solution exhibits a strong SPR band for AuNPs at 525 nm. The solution, when stirred in the dark for 24 h, scarcely changes the SPR band. As shown in Figure 5a, the transmission electron microscopy (TEM) image of the sample shows highly dispersed spherical AuNPs with an average diameter ca. 5 nm. In contrast, as shown by the black lines (Figure 4a), UV irradiation (300 nm) of the solution leads to a red-shift of the SPR band, assigned to the interparticle-coupled plasmon excitons of aggregated AuNPs.[43] TEM observations (Figure 5b−e) indeed show a formation of aggregated AuNPs, and their sizes increase with UV irradiation time. In contrast, as shown in Figure S5 (Supporting Information), UV irradiation of unmodified AuNPs shows almost no change in the SPR band. These findings suggest that the SP → MC isomerization of the surface **1** molecules promoted by UV irradiation on the AuNPs surface triggers the aggregation of AuNPs.

Figure 6a shows the change in the hydrodynamic diameter of **1**-AuNPs with UV irradiation time, determined by dynamic laser scattering (DLS) analysis. The size of AuNPs increases with irradiation time, while maintaining monodispersed

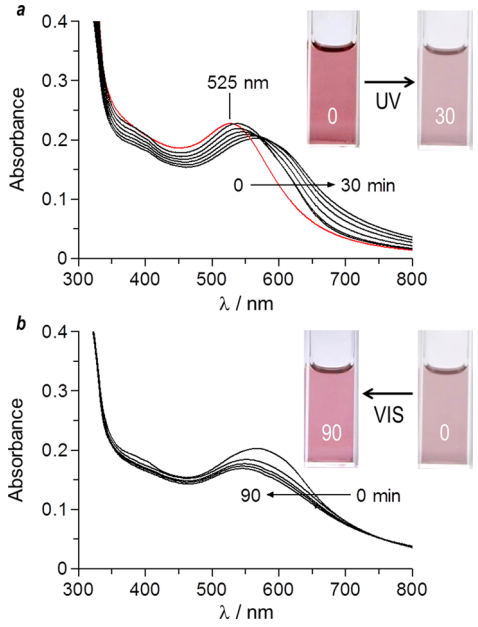

Figure 4. Absorption spectra of AuNPs (49 nM) modified with **1** (100 μM) measured in toluene upon irradiation of (a) 300 nm light and (b) 580 nm light. The red line show the spectrum obtained in the dark without photoirradiation.

distribution. As shown in Figure 6c, the size of aggregates increases from 5 to 340 nm with UV irradiation, and the aggregates maintain narrow size distributions with the standard deviations being less than 31%. These data suggest that UV irradiation successfully create AuNPs aggregates with tunable sizes and narrow size distributions.

The mechanism for aggregation of **1**-AuNPs by UV irradiation can be explained on the basis of DLVO theory involving electrostatic repulsion and van der Waals attraction between the AuNPs.[9] In the dark condition, AuNPs are well dispersed in solution due to the electrostatic repulsion between AuNPs. UV irradiation promotes SP → MC isomerization of the attached **1** molecules and increases the surface dipole moment. This decreases the energy barrier for repulsion between AuNPs and triggers their aggregation. The above mechanism is confirmed by UV irradiation of AuNPs modified with different amount of **1**. As shown in Figure S6 (Supporting Information), the aggregation rate of AuNPs increases with an increase in the amount of **1** loaded. This suggests that a larger amount of MC forms on the AuNPs surface decreases the repulsive energy barrier more easily and triggers rapid aggregation of AuNPs. The data clearly support the proposed aggregation mechanism. It must also be noted that, as shown in Figure 3c, the aggregated **1**-AuNPs obtained after UV irradiation still show 1:2 Au−S XPS signals. This suggests that the **1** molecules on the AuNPs surface remain stably even after UV irradiation.

2.4. Properties of Aggregated 1-AuNPs in the Dark Condition. The notable feature of this system is that the aggregated AuNPs, when left even in the dark condition, do not disperse and maintain their sizes. As shown in Figure 6c, the aggregated **1**-AuNPs obtained by UV irradiation for 40 min, when stirred in the dark even for a long time (72 h), shows almost the same size distributions. This suggests that the MC forms of **1** on the aggregated AuNPs remain without reversion to the SP form even in the dark condition. The retaining of the

dx.doi.org/10.1021/am5009002 | ACS Appl. Mater. Interfaces 2014, 6, 7554−7562

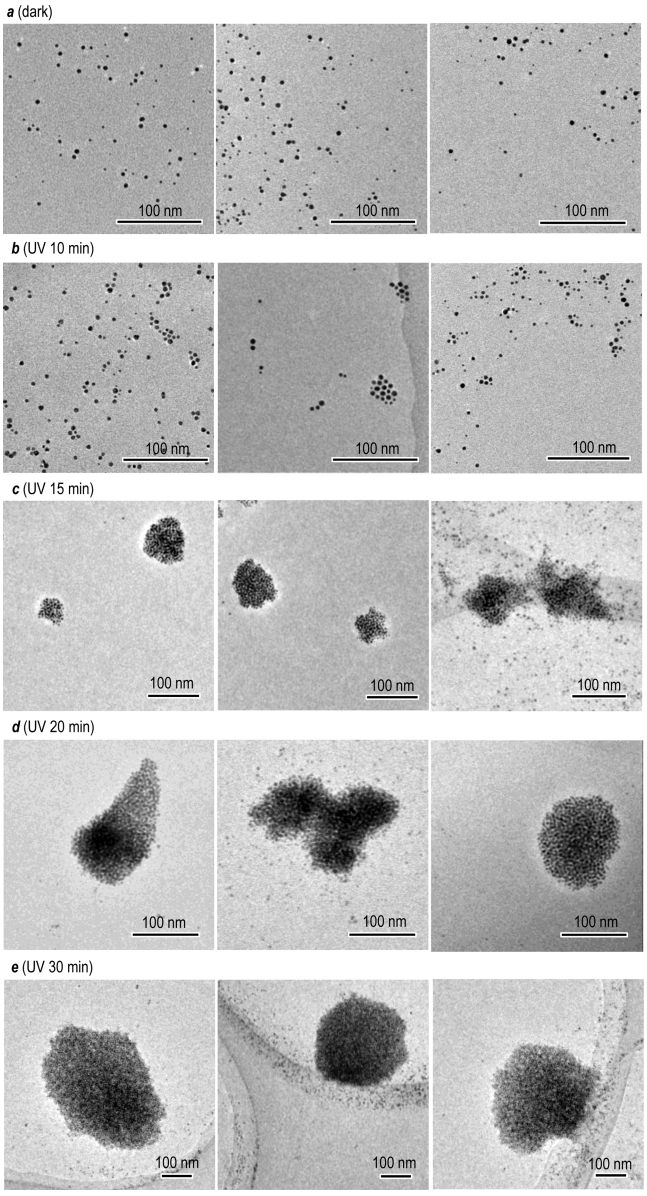

Figure 5. TEM images of **1**-AuNPs measured after stirring in toluene upon UV irradiation (300 nm). The irradiation times are (a) 0, (b) 10, (c) 15, (d) 20, and (e) 30 min, respectively. TEM samples were prepared by dipping the sample grid into the solution followed by drying in vacuo.

MC form on the AuNPs is confirmed by IR analysis. As shown in Figure 7b, the compound **1**, when irradiated by UV light, shows a characteristic band at 1353 cm^{-1}, assigned to the C–N^+ stretching vibration of the MC form.[44] In contrast, **1** measured in the dark does not show this band (Figure 7a). As shown in Figure 7d, 1-AuNPs measured without UV irradiation also show no C–N^+ band. However, as shown in Figure 7e, the aggregated **1**-AuNPs, obtained by UV irradiation (30 min) followed by stirring in the dark (2 h), shows distinctive C–N^+ band. This clearly suggests that the MC forms of **1** on the AuNPs aggregated by UV irradiation remain without reversion to the SP forms even when left in the dark condition.

As shown in Figure 1, the MC form of compound **1**, when left in the dark, undergoes thermal reversion to the SP form. This is inconsistent with the result obtained in the AuNPs system (Figure 6c). The retaining of the MC forms on the

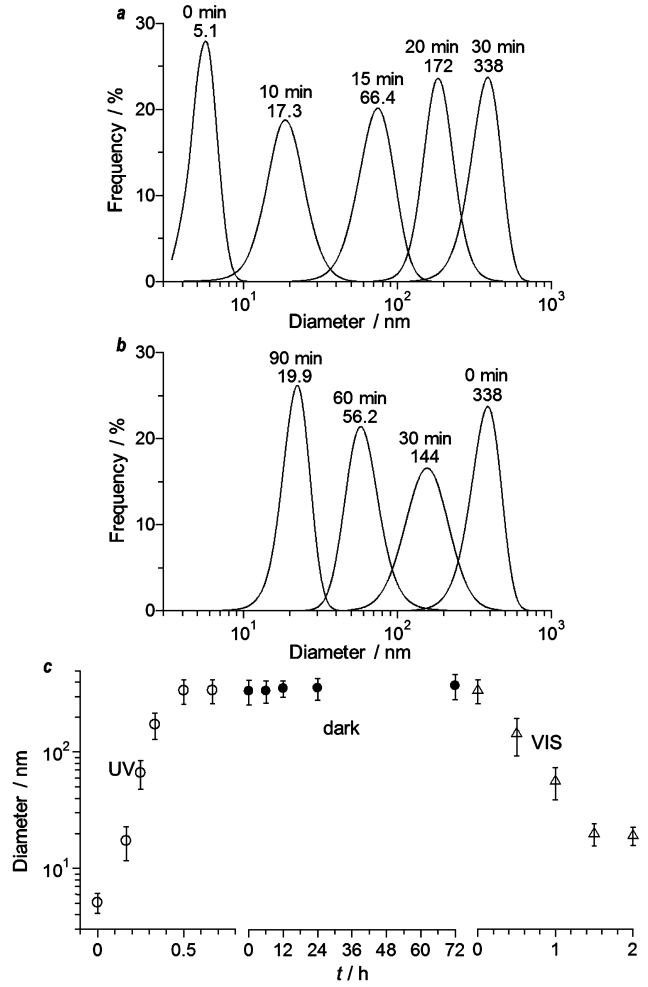

Figure 6. Time-dependent change in the hydrodynamic diameter for the aggregates of **1**-AuNPs (AuNPs, 49 nM; **1**, 100 μM) upon (a) UV (300 nm) and (b) visible light (580 nm) irradiation. (c) Change in the average diameter of aggregates during the UV, dark, and visible light irradiation sequence.

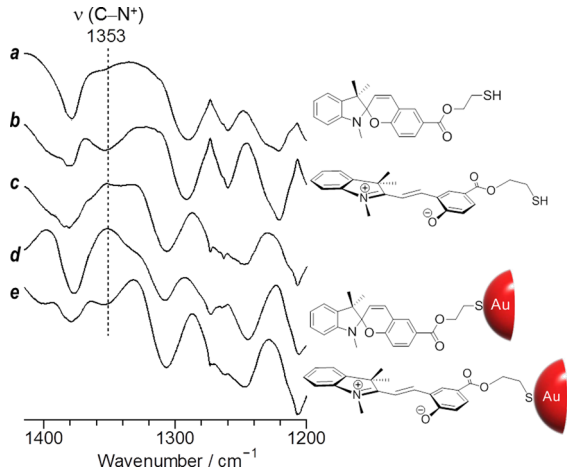

Figure 7. IR spectra for (a) SP and (b) MC forms of **1**, (c) unmodified AuNPs, (d) **1**-AuNPs measured in the dark, and (e) aggregated **1**-AuNPs obtained upon UV irradiation (300 nm, 30 min) followed by stirring in the dark for 2 h. All measurements were carried out in 1,1,1,3,3,3-hexafluoro-2-propanol.

dx.doi.org/10.1021/am5009002 | ACS Appl. Mater. Interfaces 2014, 6, 7554–7562

aggregated AuNPs is because the stacking interaction between the MC forms stabilizes the MC forms, as often observed in the systems with a large amount of spiropyran dyes.[45−48] This suppresses thermal MC → SP reversion and, hence, maintains electrostatic attractive force between the AuNPs, as observed in related spiropyran-modified AuNPs systems.[49,50] As shown in Figure S7 (Supporting Information), the rate of thermal MC → SP reversion of the compound **1** decreases with an increase in the concentration of the MC form in solution. This suggests that MC forms indeed associate with each other via the stacking interaction. In the AuNPs system, the MC forms exist on the AuNPs surface with very high density. They strongly associate via the stacking interaction and suppress thermal MC → SP reversion. This thus maintains the electrostatic attractive force between the AuNPs. In contrast, some reports[25−27] described that thermal MC → SP reversion of spiropyran-modified AuNPs does occur in aqueous media. This is because, as reported,[45−48] the stacking interaction between the MC forms strongly depends on the solvent polarity; less polar solvents such as toluene used in our system and related systems[49,50] promote efficient stacking, whereas polar solvents such as water scarcely promotes.

Figure 8 shows a typical high-resolution TEM image of the aggregated **1**-AuNPs obtained upon UV irradiation for 15 min.

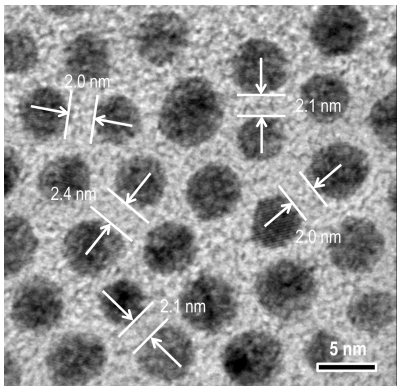

Figure 8. Typical high-resolution TEM image of aggregated **1**-AuNPs obtained upon UV irradiation (300 nm) for 15 min.

Single AuNPs are spatially aligned with similar distances. The average distances between the AuNPs are determined to be 2.1 nm. As shown in Figure 2, the head-to-tail length of the **1** molecule is determined by DFT calculation to be 1.65 nm, which is close to the distances between the AuNPs. These data suggest that, as shown in Scheme 2, the MC forms of the **1** molecules on the AuNPs surface are stabilized by the stacking interaction between AuNPs.

2.5. Dispersion of Aggregated 1-AuNPs upon Visible Light Irradiation. The aggregated **1**-AuNPs can be redispersed by visible light irradiation. Figure 4b shows the change in absorption spectra upon irradiation with 580 nm light. The SPR band for aggregated AuNPs blue-shifts with irradiation time. This indicates that MC → SP isomerization of the surface **1** molecules promoted by visible light irradiation decreases the electrostatic attractive force between the AuNPs and leads to their redispersion. As shown in Figure 9, TEM observations revealed that the size of aggregates indeed decreases with irradiation time. In addition, as shown in Figure 6b,c, DLS analysis showed that, during visible light irradiation, the aggregates maintain narrow size distribution with the standard

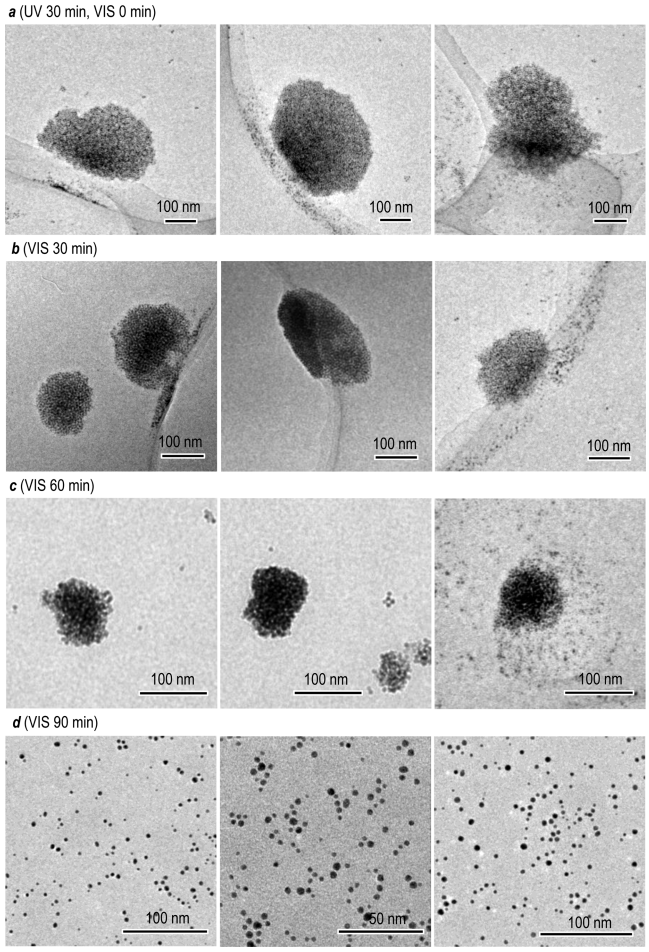

Figure 9. TEM images of aggregated **1**-AuNPs measured after stirring in toluene upon visible light irradiation (580 nm). The irradiation times are (a) 0, (b) 30, (c) 60, and (d) 90 min, respectively. The aggregated **1**-AuNPs (sample a) were prepared by 30 min UV irradition.

deviations being less than 34%. This suggests that visible light irradiation as well as UV irradiation successfully create aggregates with tunable sizes and narrow size distributions. It must also be noted that, as shown in Figure 3d, the **1**-AuNPs recovered after visible light irradiation still show 1:2 Au−S XPS signals, suggesting that the **1** molecules are stably attached on the surface even after visible light irradiation.

Figure 10a shows the change in the size of AuNPs aggregates during repeated UV/visible light irradiations. The aggregates reversibly change their sizes at least 5 cycles while maintaining narrow size distributions, suggesting that reversible size control can be attained. Figure 10b shows the change in the size of AuNPs aggregate during the dark → UV → dark → VIS cycles. The size of aggregates scarcely changes in the dark condition and can only be controlled by photoirradiation. These data suggest that UV/visible light irradiations of **1**-modified AuNPs promote reversible aggregation and dispersion, and turning off the light successfully maintains their sizes.

3. CONCLUSION

We found that spiropyran-modified AuNPs undergo reversible aggregation/dispersion by UV and visible light irradiation. The photochemical process accurately controls the size of AuNPs aggregates and produces aggregates with tunable size (20−340

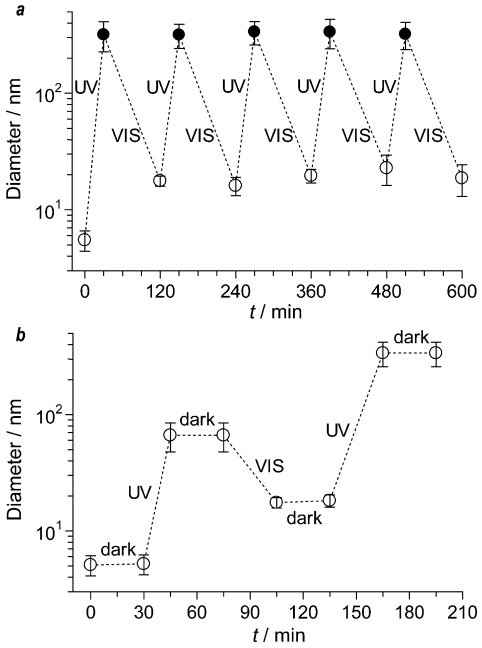

Figure 10. Time-dependent change in the hydrodynamic diameter for aggregates of **1**-AuNPs duing (a) UV (300 nm) and visible light (580 nm) irradiation sequence and (b) UV, dark, and visible light irradiation sequence.

nm) and narrow size distributions (standard deviation <34%). In contrast, the AuNPs aggregates, even when left in the dark, scarcely change their sizes. This is because the MC forms of the dyes on the AuNPs surface associate with each other via the stacking interaction. This suppresses thermal MC → SP isomerization of the dyes and maintains electrostatic attractive force between the AuNPs. The basic concept presented here, based on the photoisomerization of spiropyran, may contribute to the design of a more efficient method for light-induced self-assembly of AuNPs and may open a new strategy toward the advanced processing of metal nanoparticles.

4. EXPERIMENTAL SECTION

4.1. Materials. All reagents were supplied from Wako and Tokyo Kasei and used without further purification. Water was purified by the Milli-Q system. Compounds **2**[34] and **3**[35] were synthesized according to literature procedures.

4.2. Synthesis of 1. **2** (0.6 g, 3.5 mmol) and **3** (0.4 g, 2.4 mmol) were refluxed in EtOH (6 mL) for 8 h. The resultant was concentrated by evaporation and purified by silica gel column chromatography with CH_2Cl_2/MeOH (10/1, v/v), affording **4** as a red solid (0.52 g, 1.62 mmol, 70%). **4** (0.22 g, 0.7 mmol), EDC (0.72 g, 3.8 mmol), DMAP (0.46 g, 3.8 mmol), and 2-mercaptoethanol (78 μL, 1.1 mmol) were dissolved in $CHCl_3$ (20 mL) and stirred at room temperature for 60 h. The resultant was concentrated by evaporation. Saturated NH_4Cl solution (20 mL) was added to the residue, and the organic phase was extracted with CH_2Cl_2 (20 mL × 3). The combined organic layers were washed with brine, dried over Na_2SO_4, and concentrated by evaporation. The resultant was purified by silica gel column chromatography with ethyl acetate/*n*-hexane (1/3, v/v), affording **1** as a red solid (48.4 mg, 0.127 mmol, 18%). ^{1}H NMR (400 MHz, CD_3OD, TMS): δ (ppm) = 7.77−7.75 (m, 2H), 7.12 (t, 1H), 7.06−7.02 (m, 2H), 6.80 (t, 1H), 6.71 (d, 1H), 6.53 (d, 1H), 5.87 (d, 1H), 3.70 (t, 2H), 3.18 (t, 2H), 2.71 (s, 3H), 1.26 (s, 3H), 1.15 (s, 3H). ^{13}C NMR (101 MHz, acetone-d_6, TMS): δ (ppm) = 159.9, 137.2, 130.5, 130.1, 129.8, 128.5, 127.1, 123.8, 122.3, 121.5, 120.3, 119.9, 115.7, 107.8, 76.4, 61.7, 52.7, 32.7, 29.0, 26.2, 23.3, 20.2. EI-MS: calcd for $C_{22}H_{23}NO_3S$: 381.5. Found: m/z 381.4 (M^+). HRMS (EI^+) m/z calcd for $C_{22}H_{23}NO_3S$: 381.1399. Found: m/z 381.1472.

4.3. Analysis. Absorption spectra were measured on an UV−visible photodiode-array spectrophotometer (Shimadzu; Multispec−1500) equipped with a temperature controller, using a 10 mm path length quartz cell under aerated conditions. UV or visible light irradiation was carried out with a Xe lamp (300 W; Asahi Spectra Co. Ltd.; Max-302) equipped with 300, 540, or 580 nm band-pass filter.[51] ^{1}H and ^{13}C NMR spectra were obtained by a JEOL JNM-AL400 Excalibur using TMS as standard. EI-MS analysis was performed by a JEOL JMS 700 spectrometer. Hydrodynamic diameter of AuNPs was measured by a dynamic laser scattering spectrometer (LB-500, HORIBA).[52] TEM observations were carried out using an FEI Tecnai G2 20ST analytical electron microscope operated at 200 kV.[53] XPS analysis was performed using a Kratos Axis Ultra spectrometer with Mg Kα radiation as the energy source.[25] Infrared spectra were recorded at room temperature using a FTIR−610 spectrometer (Jasco Corp.) with a liquid sample cell with a CaF_2 window.[54]

4.4. Computational Details. Ab initio calculations were performed within the Gaussian 03 program.[39] Geometry optimization was performed with the DFT level using the B3LYP function and the 6-31G basis set. The electronic energies were calculated with TDDFT at the same level of optimization using the polarizable continuum model (PCM) with water as a solvent.

■ ASSOCIATED CONTENT

Ⓢ Supporting Information

Characterization data for compound **1** (Figures S1−S3), photoisomerization behavior of **1** (Figure S4), absorption spectra of unmodified AuNPs upon UV irradiation (Figure S5), effect of the amount of **1** on the aggregation of AuNPs (Figure S6), and thermal reversion behavior of **1** (Figure S7). This material is available free of charge via the Internet at http://pubs.acs.org.

■ AUTHOR INFORMATION

Corresponding Author

*Y. Shiraishi. E-mail: shiraish@cheng.es.osaka-u.ac.jp.

Notes

The authors declare no competing financial interest.

■ ACKNOWLEDGMENTS

This work was supported by the Grant-in Aid for Scientific Research (No. 23360349) from the Ministry of Education, Culture, Sports, Science and Technology, Japan (MEXT).

■ REFERENCES

(1) Stewart, M. E.; Anderton, C. R.; Thompson, L. B.; Maria, J.; Gray, S. K.; Rogers, J. A.; Nuzzo, R. G. Nanostructured Plasmonic Sensors. *Chem. Rev.* **2008**, *108*, 494−521.

(2) Grzelczak, M.; Vermant, J.; Furst, E. M.; Liz-Marzán, L. M. Directed Self-Assembly of Nanoparticles. *ACS Nano* **2010**, *4*, 3591−3605.

(3) Daniel, M. C.; Astruc, D. Gold Nanoparticles: Assembly, Supramolecular Chemistry, Quantum-Size-Related Properties, and Applications toward Biology, Catalysis, and Nanotechnology. *Chem. Rev.* **2004**, *104*, 293−346.

(4) Jain, P. K.; El-Sayed, I. H.; El-Sayed, M. A. Au Nanoparticles Target Cancer. *Nano Today* **2007**, *2*, 18−29.

(5) Hvolbæk, B.; Janssens, T. V. W.; Clausen, B. S.; Falsig, H.; Christensen, C. H.; Nørskov, J. K. Catalytic Activities of Au Nanoparticles. *Nano Today* **2007**, *2*, 14−18.

(6) Tsukamoto, D.; Shiraishi, Y.; Sugano, Y.; Ichikawa, S.; Tanaka, S.; Hirai, T. Gold Nanoparticles Located at the Interface of Anatase/Rutile TiO_2 Particles as Active Plasmonic Photocatalysts for Aerobic Oxidation. *J. Am. Chem. Soc.* **2012**, *134*, 6309−6315.

(7) Sugano, Y.; Shiraishi, Y.; Tsukamoto, D.; Ichikawa, S.; Tanaka, S.; Hirai, T. Supported Au−Cu Bimetallic Alloy Nanoparticles: An Aerobic Oxidation Catalyst with Regenerable Activity by Visible-Light Irradiation. *Angew. Chem., Int. Ed.* **2013**, *52*, 5295−5299.
(8) Gittins, D. I.; Bethell, D.; Schiffrin, D. J.; Nichols, R. J. A Nanometre-Scale Electronic Switch Consisting of a Metal Cluster and Redox-Addressable Groups. *Nature* **2000**, *408*, 67−69.
(9) Bishop, K. J. M.; Wilmer, C. E.; Soh, S.; Grzybowski, B. A. Nanoscale Forces and Their Uses in Self-Assembly. *Small* **2009**, *5*, 1600−1630.
(10) Nie, Z.; Petukhova, A.; Kumacheva, E. Properties and Emerging Applications of Self-Assembled Structures Made from Inorganic Nanoparticles. *Nat. Nanotechnol* **2010**, *5*, 15−25.
(11) Albanese, A.; Chan, W. C. W. Effect of Gold Nanoparticle Aggregation on Cell Uptake and Toxicity. *ACS Nano* **2011**, *5*, 5478−5489.
(12) Arruebo, M.; Fernández-Pacheco, R.; Ibarra, M. R.; Santamaría, J. Magnetic Nanoparticles for Drug Delivery. *Nano Today* **2007**, *2*, 22−32.
(13) Sidhaye, D. S.; Kashyap, S.; Sastry, M.; Hotha, S.; Prasad, B. L. V. Gold Nanoparticle Networks with Photoresponsive Interparticle Spacings. *Langmuir* **2005**, *21*, 7979−7984.
(14) Manna, A.; Chen, P. L.; Akiyama, H.; Wei, T. X.; Tamada, K.; Knoll, W. Optimized Photoisomerization on Gold Nanoparticles Capped by Unsymmetrical Azobenzene Disulfides. *Chem. Mater.* **2003**, *15*, 20−28.
(15) Raimondo, C.; Reinders, F.; Soydaner, U.; Mayor, M.; Samorì, P. Light-Responsive Reversible Solvation and Precipitation of Gold Nanoparticles. *Chem. Commun.* **2010**, *46*, 1147−1149.
(16) Klajn, R.; Wesson, P. J.; Bishop, K. J. M.; Grzybowski, B. A. Writing Self-Erasing Images using Metastable Nanoparticle "Inks". *Angew. Chem., Int. Ed.* **2009**, *48*, 7035−7039.
(17) Luo, Y.; Korchak, S.; Vieth, H. M.; Haag, R. Effective Reversible Photoinduced Switching of Self-Assembled Monolayers of Functional Imines on Gold Nanoparticles. *ChemPhysChem* **2011**, *12*, 132−135.
(18) Housni, A.; Zhao, Y.; Zhao, Y. Using Polymers To Photoswitch the Aggregation State of Gold Nanoparticles in Aqueous Solution. *Langmuir* **2010**, *26*, 12366−12370.
(19) Klajn, R.; Bishop, K. J. M.; Grzybowski, B. A. Light-controlled Self-Assembly of Reversible and Irreversible Nanoparticle Supra-structures. *Proc. Natl. Acad. Sci. U. S. A.* **2007**, *104*, 10305−10309.
(20) Klajn, R.; Browne, K. P.; Soh, S.; Grzybowski, B. A. Nanoparticles That "Remember" Temperature. *Small* **2010**, *6*, 1385−1387.
(21) Zhou, J.; Sedev, R.; Beattie, D.; Ralston, J. Light-Induced Aggregation of Colloidal Gold Nanoparticles Capped by Thymine Derivatives. *Langmuir* **2008**, *24*, 4506−4511.
(22) Itoh, H.; Tahara, A.; Naka, K.; Chujo, Y. Photochemical Assembly of Gold Nanoparticles Utilizing the Photodimerization of Thymine. *Langmuir* **2004**, *20*, 1972−1976.
(23) Lai, J.; Xu, Y.; Mu, X.; Wu, X.; Li, C.; Zheng, J.; Wu, C.; Chen, J.; Zhao, Y. Light-Triggered Covalent Assembly of Gold Nanoparticles in Aqueous Solution. *Chem. Commun.* **2011**, *47*, 3822−3824.
(24) Shiraishi, Y.; Tanaka, K.; Shirakawa, E.; Sugano, Y.; Ichikawa, S.; Tanaka, S.; Hirai, T. Light-Triggered Self-Assembly of Gold Nanoparticles Based on Photoisomerization of Spirothiopyran. *Angew. Chem., Int. Ed.* **2013**, *52*, 8304−8308.
(25) Ipe, B. I.; Mahima, S.; Thomas, K. G. Light-Induced Modulation of Self-Assembly on Spiropyran-Capped Gold Nanoparticles: A Potential System for the Controlled Release of Amino Acid Derivatives. *J. Am. Chem. Soc.* **2003**, *125*, 7174−7175.
(26) Liu, D.; Chen, W.; Sun, K.; Deng, K.; Zhang, W.; Wang, Z.; Jiang, X. Resettable, Multi-Readout Logic Gates Based on Controllably Reversible Aggregation of Gold Nanoparticles. *Angew. Chem., Int. Ed.* **2011**, *50*, 4103−4107.
(27) Osborne, E. A.; Jarrett, B. R.; Tu, C.; Louie, A. Y. Modulation of T2 Relaxation Time by Light-Induced, Reversible Aggregation of Magnetic Nanoparticles. *J. Am. Chem. Soc.* **2010**, *132*, 5934−5935.
(28) Wei, Y.; Han, S.; Kim, J.; Soh, S.; Grzybowski, B. A. Photoswitchable Catalysis Mediated by Dynamic Aggregation of Nanoparticles. *J. Am. Chem. Soc.* **2010**, *132*, 11018−11020.
(29) Brown, G. H. *Photochromism*; *Techniques of Chemistry*, Vol. 3; Wiley-Interscience: New York, 1971.
(30) Durr, H.; Bouas-Laurent, H. *Photochromism - Molecules and Systems*; Elsevier: Amsterdam, 1990.
(31) Crano, J. C.; Guglielmetti, R. J. *Organic Photochromic and Thermochromic Compounds*; Plenum Press: New York, 1999.
(32) Klajn, R. Spiropyran-Based Dynamic Materials. *Chem. Soc. Rev.* **2014**, *43*, 148−184.
(33) Keum, S.-R.; Hur, M.-S.; Kazmaier, P. M.; Buncel, E. Thermo- and Photochromic Dyes: Indolino-benzospiropyrans. Part I. UV-VIS Spectroscopic Studies of 1,3,3-spiro(2*H*-1-benzopyran-2,2′-indolines) and the Open-Chain Merocyanine Forms; Solvatochromism and Medium Effects on Spiro Ring Formation. *Can. J. Chem.* **1991**, *69*, 1940−1947.
(34) Shiraishi, Y.; Adachi, K.; Itoh, M.; Hirai, T. Spiropyran as a Selective, Sensitive, and Reproducible Cyanide Anion Receptor. *Org. Lett.* **2009**, *11*, 3482−3485.
(35) Wynberg, H. Some Observations on the Mechanism of the Reimer-Tiemann Reaction. *J. Am. Chem. Soc.* **1954**, *76*, 4998−4999.
(36) Shiraishi, Y.; Inoue, T.; Sumiya, S.; Hirai, T. Entropy-Driven Thermal Isomerization of Spiropyran in Viscous Media. *J. Phys. Chem. A* **2011**, *115*, 9083−9090.
(37) Heller, C. A.; Fine, D. A.; Henry, R. A. Photochromism. *J. Phys. Chem.* **1961**, *65*, 1908−1909.
(38) Shiraishi, Y.; Miyamoto, R.; Hirai, T. Spiropyran-Conjugated Thermoresponsive Copolymer as a Colorimetric Thermometer with Linear and Reversible Color Change. *Org. Lett.* **2009**, *11*, 1571−1574.
(39) Frisch, M. J.; Trucks, G. W.; Schlegel, H. B.; Scuseria, G. E.; Robb, M. A.; Cheeseman, Jr. J. R.; Montgomery, J. A.; Vreven, T.; Kudin, K. N.; Burant, J. C.; Millam, J. M.; Iyengar, S. S.; Tomasi, J.; Barone, V.; Mennucci, B.; Cossi, M.; Scalmani, G.; Rega, N.; Petersson, G. A.; Nakatsuji, H.; Hada, M.; Ehara, M.; Toyota, K.; Fukuda, R.; Hasegawa, J.; Ishida, M.; Nakajima, T.; Honda, Y.; Kitao, O.; Nakai, H.; Klene, M.; Li, X.; Knox, J. E.; Hratchian, H. P.; Cross, J. B.; Bakken, V.; Adamo, C.; Jaramillo, J.; Gomperts, R.; Stratmann, R. E.; Yazyev, O.; Austin, A. J.; Cammi, R.; Pomelli, C.; Ochterski, J. W.; Ayala, P. Y.; Morokuma, K.; Voth, G. A.; Salvador, P.; Dannenberg, J. J.; Zakrzewski, V. G.; Dapprich, S.; Daniels, A. D.; Strain, M. C.; Farkas, O.; Malick, D. K.; Rabuck, A. D.; Raghavachari, K.; Foresman, J. B.; Ortiz, J. V.; Cui, Q.; Baboul, A. G.; Clifford, S.; Cioslowski, J.; Stefanov, B. B.; Liu, G.; Liashenko, A.; Piskorz, P.; Komaromi, I.; Martin, R. L.; Fox, D. J.; Keith, T.; Al-Laham, M. A.; Peng, C. Y.; Nanayakkara, A.; Challacombe, M.; Gill, P. M. W.; Johnson, B.; Chen, W.; Wong, M. W.; Gonzalez, C.; Pople, J. A. *Gaussian 03*, Revision B.05; Gaussian, Inc.: Wallingford, CT, 2004.
(40) Brust, M.; Walker, M.; Bethell, D.; Schiffrin, D. J.; Whyman, R. Synthesis of Thiol-derivatised Gold Nanoparticles in a Two-phase Liquid-Liquid System. *J. Chem. Soc., Chem. Commun.* **1994**, 801−802.
(41) Castner, D. G.; Hinds, K.; Grainger, D. W. X-ray Photoelectron Spectroscopy Sulfur 2p Study of Organic Thiol and Disulfide Binding Interactions with Gold Surfaces. *Langmuir* **1996**, *12*, 5083−5086.
(42) Sun, S.; Mendes, P.; Critchley, K.; Diegoli, S.; Hanwell, M.; Evans, S. D.; Leggett, G. J.; Preece, J. A.; Richardson, T. H. Fabrication of Gold Micro- and Nanostructures by Photolithographic Exposure of Thiol-Stabilized Gold Nanoparticles. *Nano Lett.* **2006**, *6*, 345−350.
(43) Jain, P. K.; Huang, W.; El-Sayed, M. A. On the Universal Scaling Behavior of the Distance Decay of Plasmon Coupling in Metal Nanoparticle Pairs: A Plasmon Ruler Equation. *Nano Lett.* **2007**, *7*, 2080−2088.
(44) Fries, K. H.; Driskell, J. D.; Samanta, S.; Locklin, J. Spectroscopic Analysis of Metal Ion Binding in Spiropyran Containing Copolymer Thin Films. *Anal. Chem.* **2010**, *82*, 3306−3314.
(45) Kalisky, Y.; Williams, D. J. Laser Photolysis Studies of Photoinduced Aggregation in Polymers Containing Spiropyran Units. *Macromolecules* **1984**, *17*, 292−296.

(46) Goldburt, E.; Shvartsman, F.; Krongauz, V. "Zipper" Crystallization of Polymers with Spiropyran Side Groups. *Macromolecules* **1984**, *17*, 1876−1878.
(47) Goldburt, E.; Shvartsman, F.; Fishman, S.; Krongauz, V. Intramolecular Interactions in Photochromic Spiropyran-Merocyanine Polymers. *Macromolecules* **1984**, *17*, 1225−1230.
(48) Cabrera, I.; Krongauz, V. Physical Cross-Linking of Mesomorphic Polymers Containing Spiropyran Groups. *Macromolecules* **1987**, *20*, 2713−2717.
(49) Ma, L.; Li, J.; Han, D.; Geng, H.; Chen, G.; Li, Q. Synthesis of Photoresponsive Spiropyran-Based Hybrid Polymers and Controllable Light-Triggered Self-Assembly Study in Toluene. *Macromol. Chem. Phys.* **2013**, *214*, 716−725.
(50) Bell, N. S.; Piech, M. Photophysical Effects between Spirobenzopyran-Methyl methacrylate-Functionalized Colloidal Particles. *Langmuir* **2006**, *22*, 1420−1427.
(51) Shiraishi, Y.; Sumiya, S.; Hirai, T. Highly Sensitive Cyanide Anion Detection with a Coumarin-Spiropyran Conjugate as a Fluorescent Receptor. *Chem. Commun.* **2011**, *47*, 4953−4955.
(52) Koizumi, H.; Shiraishi, Y.; Tojo, S.; Fujitsuka, M.; Majima, T.; Hirai, T. Temperature-Driven Oxygenation Rate Control by Polymeric Photosensitizer. *J. Am. Chem. Soc.* **2006**, *128*, 8751−8753.
(53) Shiraishi, Y.; Sakamoto, H.; Sugano, Y.; Ichikawa, S.; Hirai, T. Pt-Cu Bimetallic Alloy Nanoparticles Supported on Anatase TiO_2: Highly Active Catalysts for Aerobic Oxidation Driven by Visible Light. *ACS Nano* **2013**, *7*, 9287−9297.
(54) Shiraishi, Y.; Matsunaga, Y.; Hirai, T. Selective Colorimetric Sensing of Co(II) in Aqueous Media with a Spiropyran−Amide−Dipicolylamine Linkage under UV Irradiation. *Chem. Commun.* **2012**, *48*, 5485−5487.